SUPPORTING INFORMATION FOR:

Tuning sizes, morphologies, and magnetic properties of mono- *vs.* multi-core iron oxide nanoparticles through the controlled addition of water in the polyol synthesis

Gauvin Hemery[a], Anthony C. Keyes Jr.[a], Eneko Garaio[b]*, Irati Rodrigo[b,c], Jose Angel Garcia[c,d], Fernando Plazaola[b], Elisabeth Garanger[a], Olivier Sandre[a]*

[a] LCPO, CNRS UMR 5629/ Univ. Bordeaux/ Bordeaux-INP, ENSCBP 16 avenue Pey Berland, 33607 Pessac, France

[b] Elektrizitatea eta Elektronika Saila, UPV/EHU, 48940 Leioa, Spain

[c] BCMaterials, Parque Tecnológico de Bizkaia, Ed. 50, 48160 Derio, Spain

[d] Fisika Aplikatua II Saila, UPV/EHU, 48940 Leioa, Spain

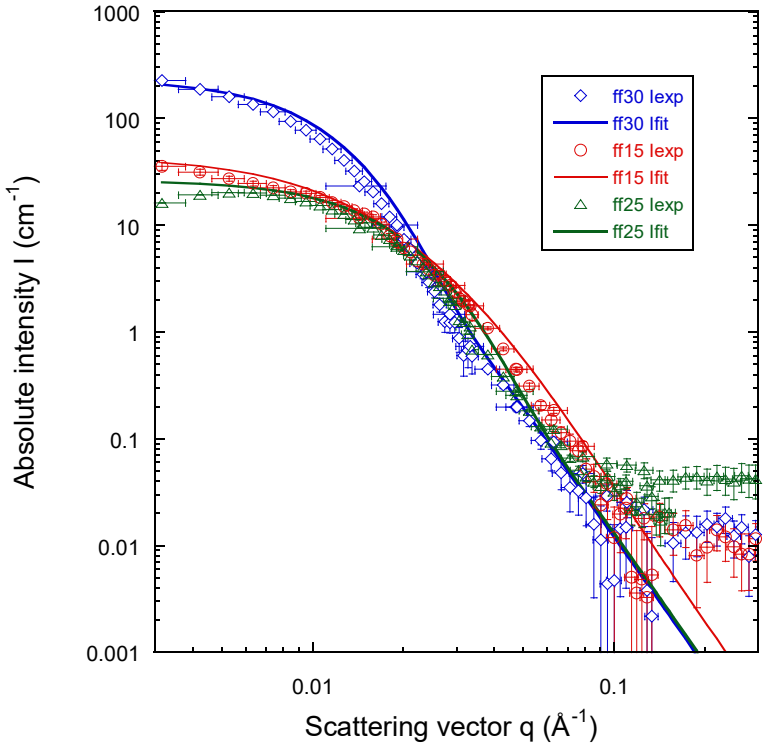

Figure S1. Small angle neutron scattering curves of samples 3off (nanoflowers), 15ff (nanoflowers) and 25ff (smooth spheres). Solid lines represent fits with polydisperse sphere form factor corresponding to following values of the intensity-average radius determined by SANS, to compare with the gyration radius by SANS and the radius obtained by TEM analysis. The specific area was estimated by the Porod law describing the intensity in the high q region: $\left[I(q) - I_{\text{background}}\right] \cdot q^4 = 2\pi\phi(1-\phi)(\Delta SLD)^2 \cdot A_{\text{spe}}$ where $\Delta SLD = 7.53 \cdot 10^{10}$ cm^{-2} stands for the neutron scattering contrast, *i.e.* the difference of scattering length density (*SLD*) calculated between the IONPs made of γ-Fe_2O_3 ($6.97 \cdot 10^{10}$ cm^{-2}) that represent a volume fraction ϕ, and the aqueous medium ($-5.6 \cdot 10^{9}$ cm^{-2} for light water). The experimental specific area A_{spe} (cm^2/cm^3) or A_{spe}/ρ (cm^2/g) can be compared to the theoretical value calculated for smooth spheres of radius R_{SANS} and volumetric mass density ρ=5 g·cm^{-3}, $A_{\text{spe}}^{\text{the}} = 3/R_{\text{SANS}}/\rho$.

3off: R_G=18.9 nm, R_{SANS}=18.1 ± 3.9 nm, R_{TEM}=23.5 ± 4.2 nm, A_{spe}=31.7 m^2·g^{-1}. $A_{\text{spe}}^{\text{the}}$=33.1 m^2·g^{-1}.

15ff: R_G=19.0 nm, R_{SANS}=10.6 ± 1.8 nm, R_{TEM}=17.5 ± 2.4 nm, A_{spe}=89.9 m^2·g^{-1} $A_{\text{spe}}^{\text{the}}$=56.6 m^2·g^{-1}.

25ff: R_G=10.5 nm, R_{SANS}=10.4 ± 2.3 nm, R_{TEM}=7.1 ± 1.6 nm, A_{spe}=52.6 m^2·g^{-1} $A_{\text{spe}}^{\text{the}}$=57.7 m^2·g^{-1}.

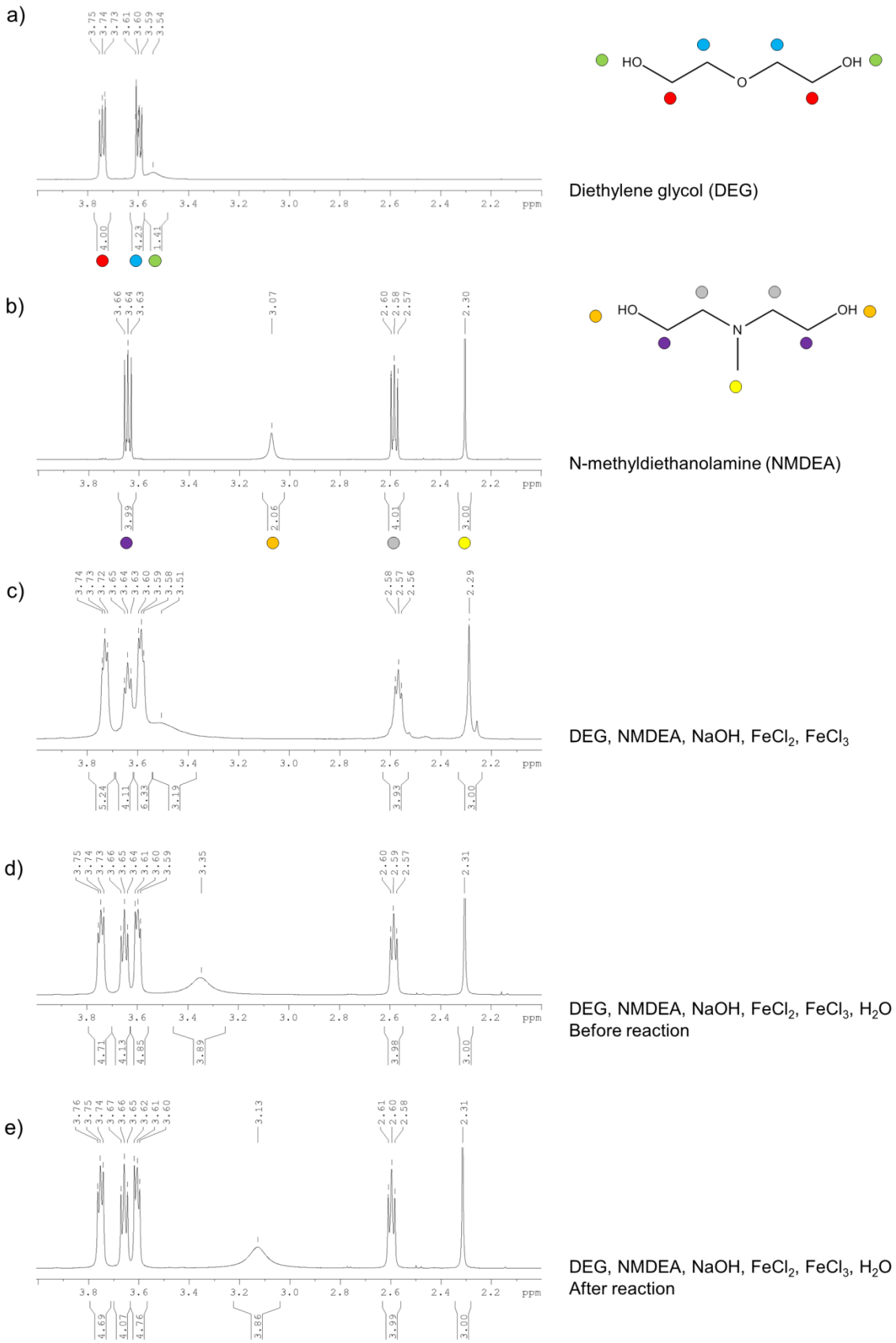

Figure S2. NMR analyses of DEG (a), NMDEA (b) and of the medium of synthesis before addition of water (c), after addition of water (d) and after reaction (e). Addition of water shifts the peak corresponding to hydroxyls, which is further shifted after reaction, possibly because of a variation of pH. The solvents do not undergo degradation during the reaction.

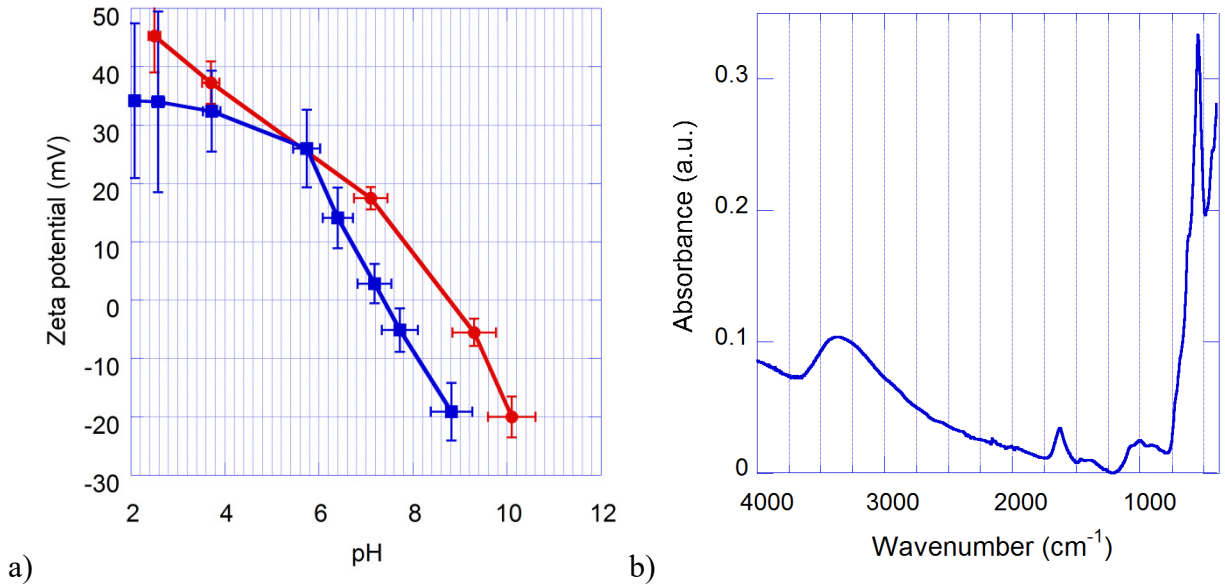

Figure S3. a) Zeta (ζ) potential measurement of IONPs whose surface is partially cleaned after the polyol synthesis (red circles), with an isoelectric point (IEP) estimated to be at around pH=9, evidencing the presence of amine moieties of NMEDEA of the solvent molecules chelated on the IONPs. When fully cleaned (blue squares), IONPs show an IEP estimated around pH=7, which is consistent with values previously reported for a bare surface of iron oxide NPs (*i.e.* coated only with neutral hydroxyl groups); b) ATR-IR spectrum of IONPs after washings (batch 21ff) presenting a broad peak in the 3000-3500 cm^{-1} range attributed to stretching vibrations of water. The bending vibration of water produces a peak at 1650 cm^{-1}, and the stretching vibration of the bond between oxygen and iron corresponds to the strong peak starting at 540 cm^{-1}. This evidences that the material is composed of iron oxide with water adsorbed, but no remaining traces of organic residues, that would yield CH_2 bands near 2800-2900 cm^{-1}.

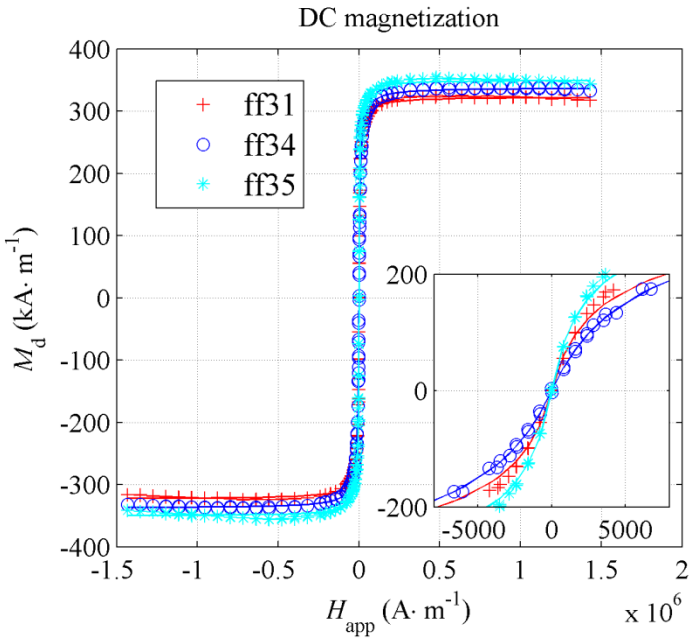

Figure S4. DC magnetization of samples 31ff, 34ff and 35ff measured by VSM. As the inset shows, they follow a superparamagnetic behavior. The signal was normalized by volume fraction calculated from the iron oxide concentration (assuming a mass density of 5 $g{\cdot}cm^3$) in order to derive the specific magnetization per domain, denominated M_d. In the linear region described by $M_d=\chi{\cdot}H_{app}$, (*i.e.* in a narrow range -1.6< H_{app}<1.6 $kA{\cdot}m^{-1}$, the susceptibility value varies between χ=45 (ff34), χ=68 (ff31) and up to χ=100 (ff35).

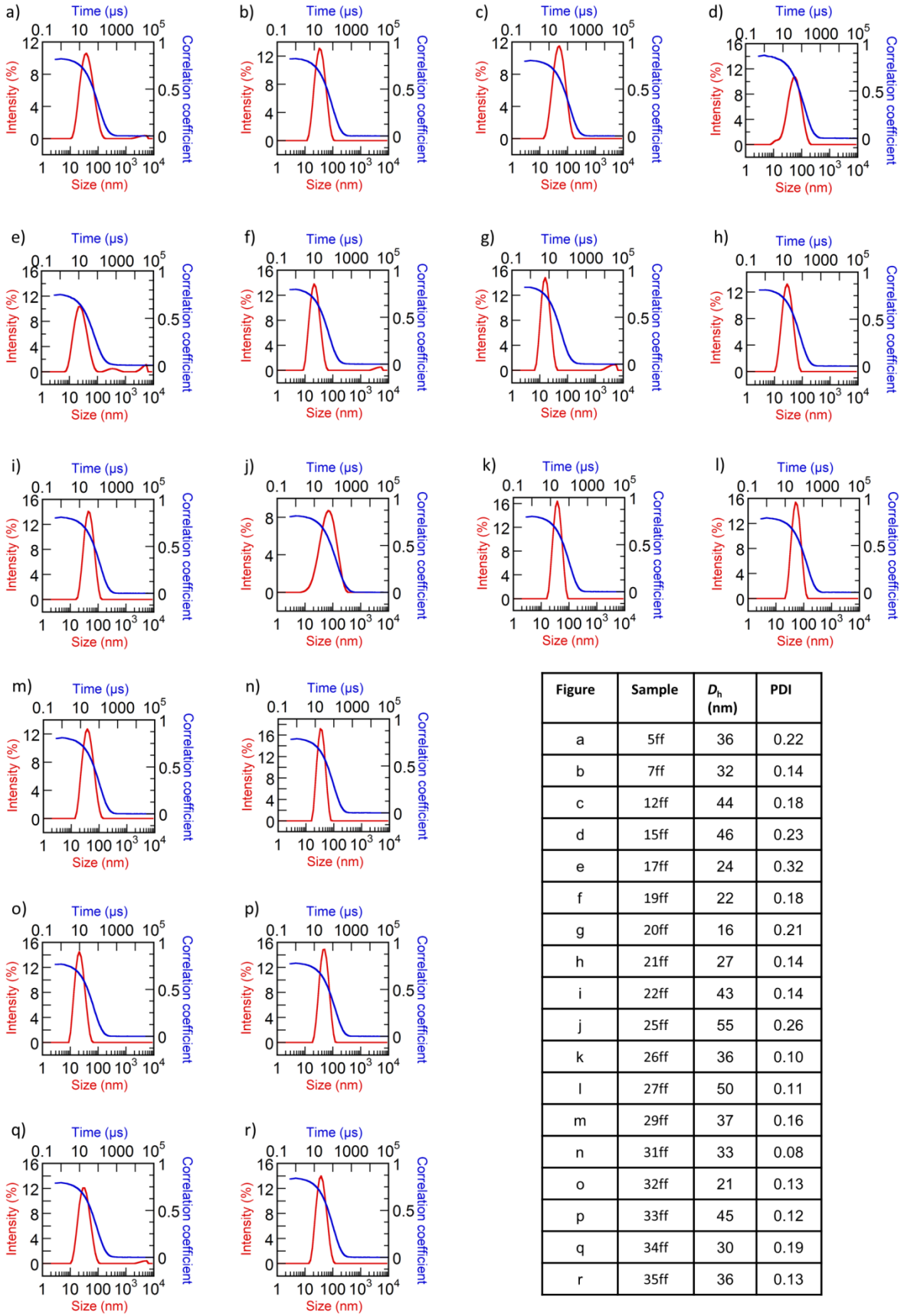

Figure	Sample	D_h (nm)	PDI
a	5ff	36	0.22
b	7ff	32	0.14
c	12ff	44	0.18
d	15ff	46	0.23
e	17ff	24	0.32
f	19ff	22	0.18
g	20ff	16	0.21
h	21ff	27	0.14
i	22ff	43	0.14
j	25ff	55	0.26
k	26ff	36	0.10
l	27ff	50	0.11
m	29ff	37	0.16
n	31ff	33	0.08
o	32ff	21	0.13
p	33ff	45	0.12
q	34ff	30	0.19
r	35ff	36	0.13

Figure S5. DLS correlograms and intensity-averaged distributions of diameters. The 2nd order cumulant fit leads to the *Z*-average hydrodynamic diameter (D_h)and polydispsersity index (PDI).

Table S1. Summary of characteristics of the sample library synthesised by the polyol route: mean diameter d_o and standard deviation σ obtained by particle counting on TEM images of N>100 IONPs on (figures in parentheses correspond to the inner core size of nanoflowers when it can be measured; an asterisk indicates a lower statistics); the initial temperature slope during 5 s under an AMF H_{app}=10.2 kA·m^{-1} at f=755 kHz and at 3 g·L^{-1} iron oxide; the specific absorption rate (normalized by the mass of iron oxide); the Z-average hydrodynamic diameter (D_h) and polydispersity index (PDI), the r_1 and r_2 relaxivities and their ratio (measured at 37°C and under 1.41 Tesla). *Lines in italics correspond to nanoflowers* (otherwise nanospheres). **Bold lines indicate samples analysed in details in main text**. Missing values correspond to measurements that were not performed because samples were estimated not interesting enough, or because of absence of colloidal stability due to a too large TEM size (*e.g.* 9ff).

Sample	$d_0 \pm \sigma$ (nm)	T slope (°C·s^{-1})	SAR (W·g^{-1})	D_h (nm)	PDI	r_1 (s^{-1}· mM$_{Fe}^{-1}$)	r_2 (s^{-1}· mM$_{Fe}^{-1}$)	r_2/r_1
4ff	8.3±1.9	-	-	-	-	12.1	113.3	9.3
5ff	*21.4±3*	*0.080*	*111*	*36.3*	*0.22*	*5.7*	*80.3*	*14.0*
7ff	7.1±1.6*	0.022	31	32.0	0.14	18.3	170.6	9.3
9ff	*60.0±7.4*	-	-	-	-	-	-	-
12ff	10.0±2	0.052	72	44.2	0.18	22.0	149.6	6.8
13ff	*11.7±4.7**	*0.14*	*189*	*57.2*	*0.35*	*15.6*	*291.3*	*18.7*
15ff	***36.9±4.8 (7.4±1.4)***	**-**	***296***	***46.3***	***0.227***	**-**	**-**	**-**
16ff	4.7±1.2	-	-	29.3	0.39	6.4	23.9	3.8
17ff	4.3±1.1	0.004	6	25.2	0.36	-	-	-
18ff	3.4±0.8	0.006	8	44.2	0.96	5.5	12.1	2.2
19ff	7.7±1.7	0.070	98	21.5	0.18	-	-	-
20ff	6.3±1.6	0.016	22	16.2	0.21	-	-	-
21ff	11.2±1.9	0.060	84	26.9	0.14	17.9	145.3	8.1
22ff	12.1±3.1	0.14	189	42.8	0.14	10.6	118.5	11.2
25ff	14.2±3.2	0.090	125	55.2	0.26	19.7	267.7	13.6
26ff	-	*0.088*	*123*	*35.7*	*0.10*	*16.0*	*219.1*	*13.7*
27ff	-	*0.11*	*150*	*49.6*	*0.11*	*12.5*	*194.2*	*15.5*
29ff	*25.9±4.5 (12.1±1.9)*	*0.13*	*178*	*36.5*	*0.16*	-	-	-
31ff	***27.5±4.2***	***0.19***	***268***	***33.3***	***0.08***	***13.1***	***341.9***	***26.1***
32ff	14.5±3.4	0.096	134	20.6	0.13	25.9	203.4	7.8
33ff	21.6±5.5	0.10	145	44.7	0.12	5.9	140.6	23.8
34ff	**32.3±5.0**	**0.15**	**206**	**29.9**	**0.19**	**12.2**	**163.1**	**13.4**
35ff	***29.1±4.4***	***0.19***	***265***	***35.7***	***0.13***	***6.2***	***170.0***	***27.3***
36ff	*32.3±5.0*	*0.17*	*237*	*71.0*	*0.37*	*0.86*	*22.3*	*25.9*

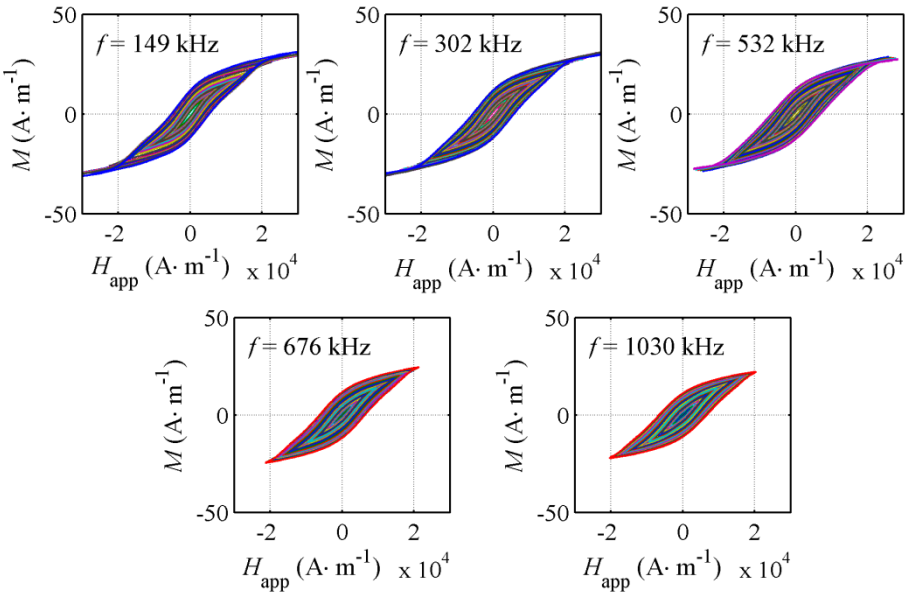

Figure S6. AC hysteresis cycles of oxidized 15ff sample (nanoflowers of grain size 7.4±1.4 nm and outer diameter 36.9±4.8 nm) at different AMF amplitudes H_{app} and frequencies (f). The superimposed black line is the DC magnetization measured by VSM.

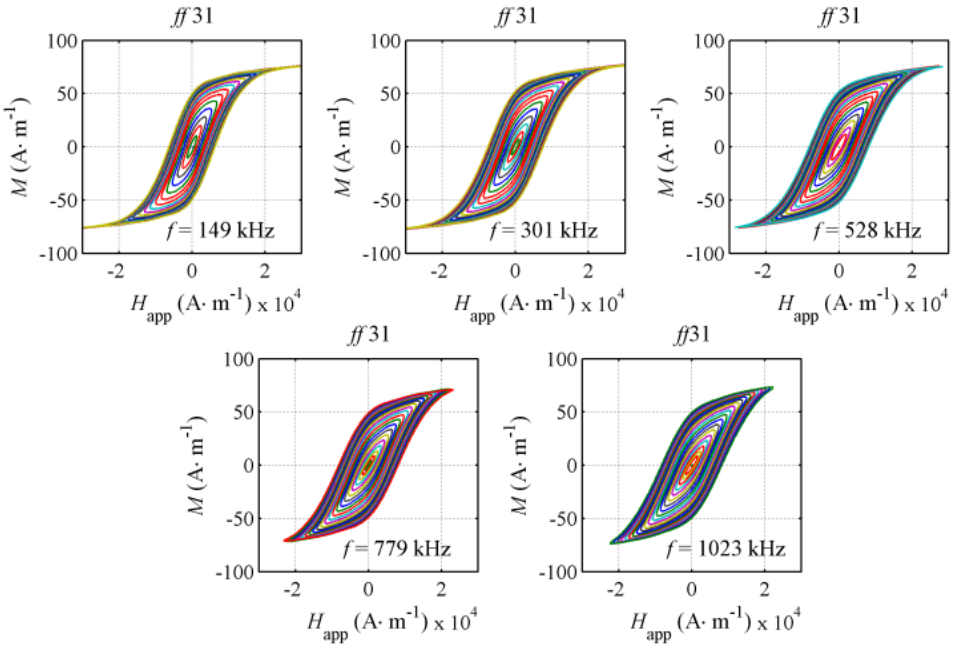

Figure S7. AC hysteresis cycles of 31ff sample (nanoflowers of 27.5 ± 4.2 nm outer diameter) at different field amplitudes H_{app} and frequencies (f).

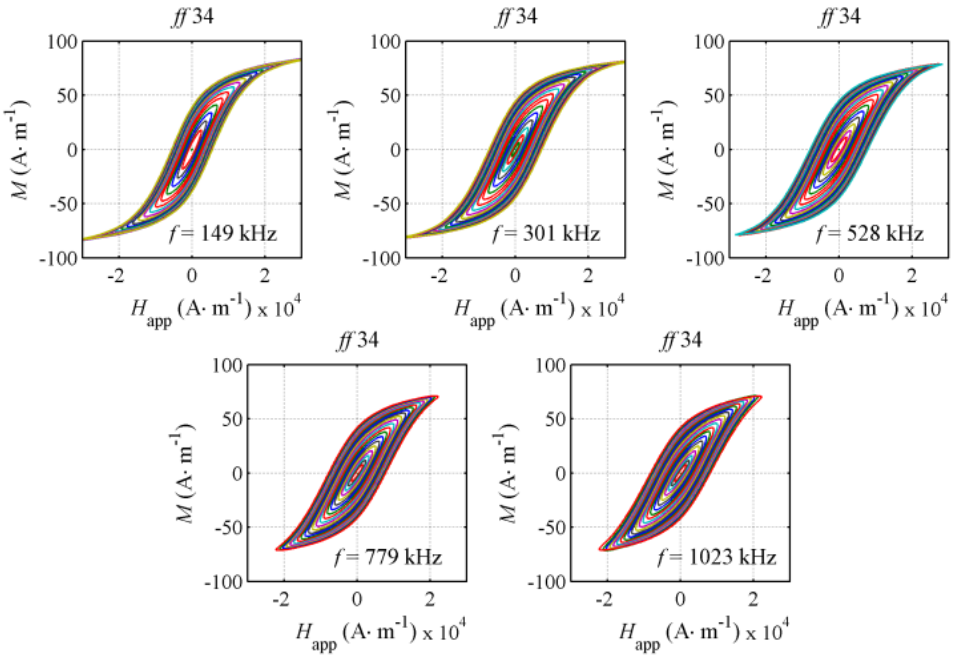

Figure S8. AC hysteresis cycles of 34ff sample (smooth nanospheres of 18.5 ± 3.2 nm diameter) at different field amplitudes H_{app} and frequencies (f).

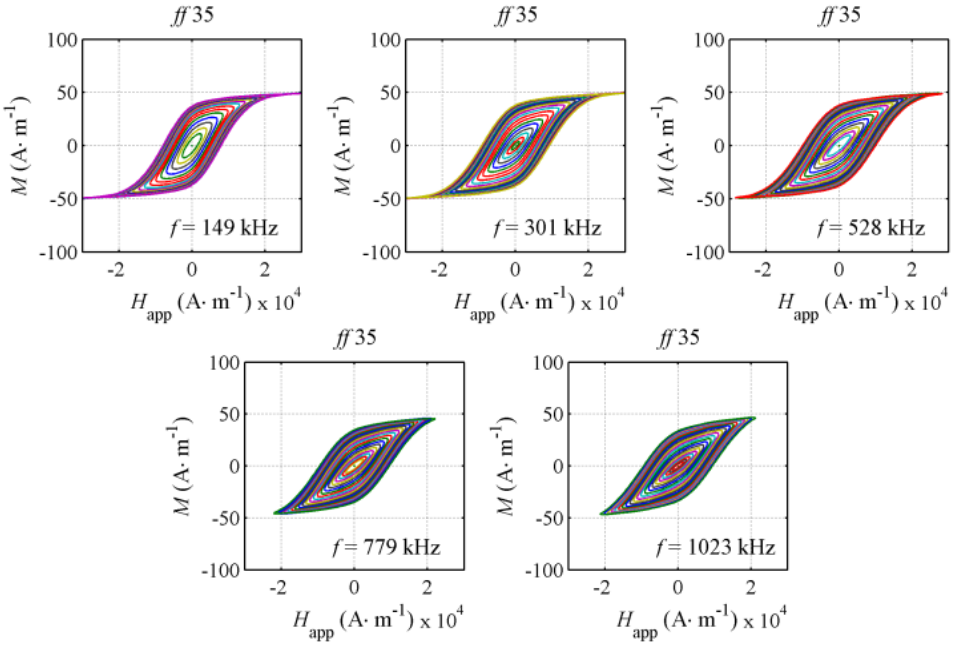

Figure S9. AC hysteresis cycles of 35ff sample (nanoflowers of 29.1 ± 4.4 nm outer diameter) at different field amplitudes H_{app} and frequencies (f).

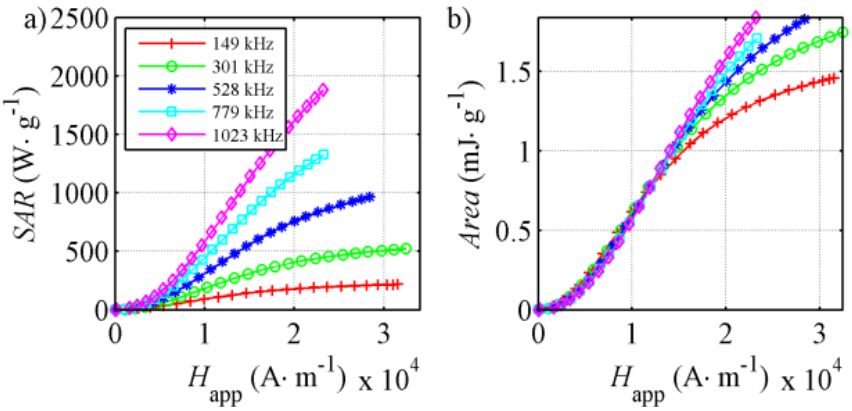

Figure S10. *SAR* (a) and hysteresis area (b) of sample 31ff (nanoflowers of 27.5 ± 4.2 nm outer diameter) *versus* applied magnetic field amplitude (H_{app}).

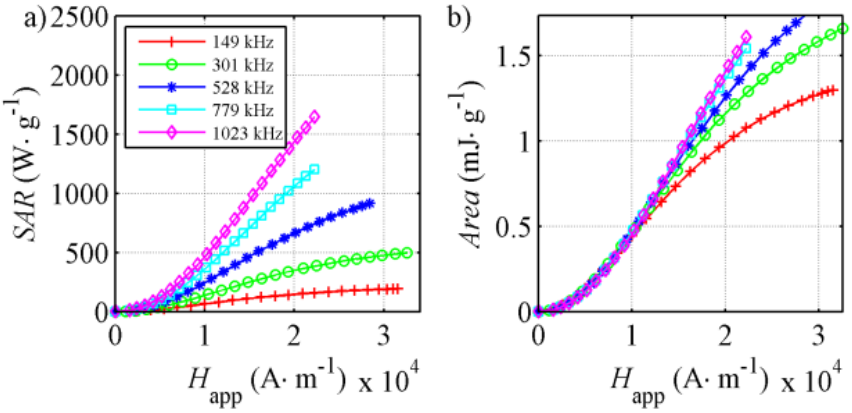

Figure S11. *SAR* (a) and hysteresis area (b) of sample 34ff (smooth nanospheres of 18.5 ± 3.2 nm diameter) *versus* applied magnetic field amplitude (H_{app}).

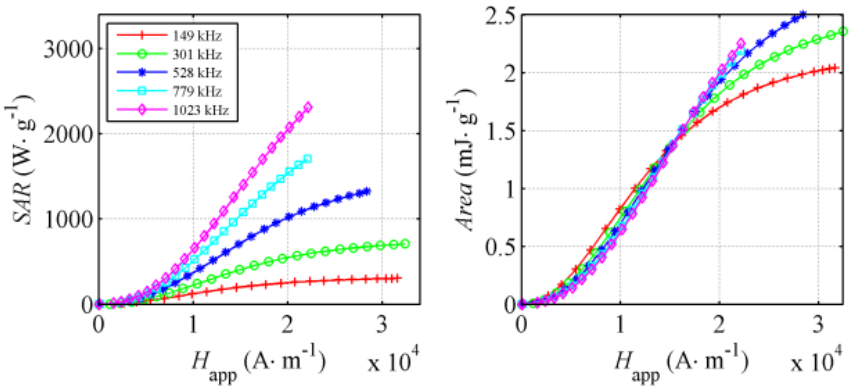

Figure S12. *SAR* (a) and hysteresis area (b) of sample 35ff (nanoflowers of 29.1 ± 4.4 nm outer diameter) *versus* applied magnetic field amplitude (H_{app}).

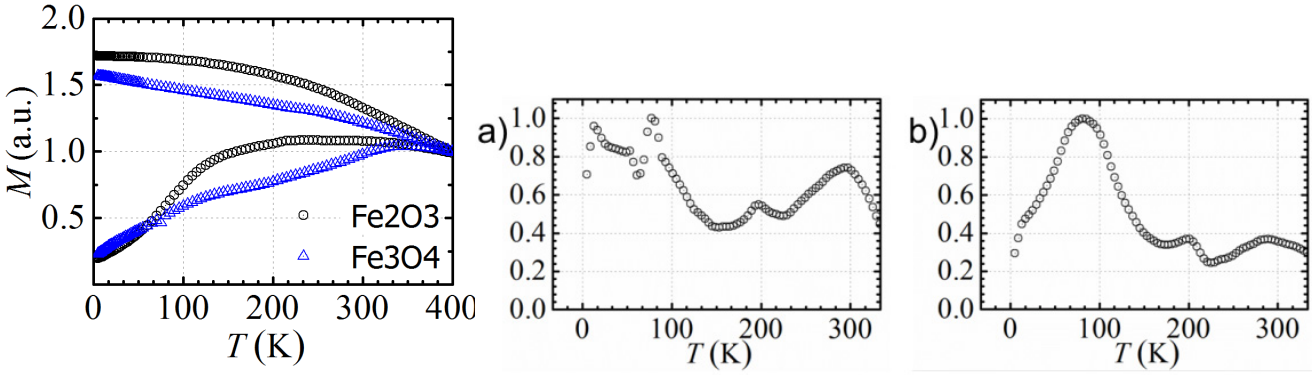

Figure S13. ZFC-FC measurement by MPMS magnetometry and derivative $d(M_{FC}-M_{ZFC})/dT$ of the FC-ZFC curve difference for un-oxidized Fe_3O_4 (a) and oxidized γ-Fe_2O_3 (b) 15ff nanoflowers. The peak near 90K is ascribed to the Verwey transition.

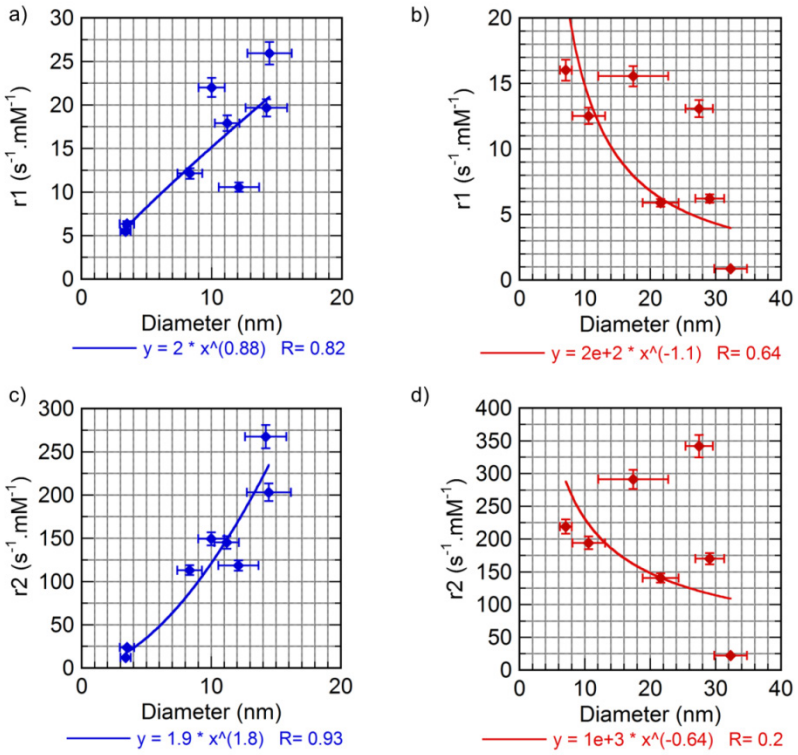

Figure S14. Longitudinal relaxivity of smooth spheres (a) and nanoflowers (b). Transverse relaxivity of smooth spheres (c) and nanoflowers (d). All measurements were performed at 37°C on a 1.41 Tesla / 60 MHz Bruker mq60 relaxometer.